Thermochimica Acta 488 (2009) 60–65

Contents lists available at ScienceDirect

Thermochimica Acta

journal homepage: www.elsevier.com/locate/tca

Crystallization and sintering characteristics of $CaO–Al_2O_3–SiO_2$ glasses in the presence of TiO_2, CaF_2 and ZrO_2

S. Banijamali*, B. Eftekhari Yekta, H.R. Rezaie, V.K. Marghussian

Ceramic Division, Department of Materials Engineering, Iran University of Science & Technology, Narmak, Tehran, Iran

ARTICLE INFO

Article history:
Received 2 July 2008
Received in revised form 17 December 2008
Accepted 20 December 2008
Available online 15 January 2009

Keywords:
Glass–ceramics
Sinterability
Crystallization

ABSTRACT

In this study, the effects of different amounts of TiO_2, ZrO_2 and CaF_2 nucleating agents on sinterability, crystallization, mechanical properties and chemical resistance of glass–ceramics belonging to the $CaO–Al_2O_3–SiO_2$ system were investigated, using differential thermal analysis (DTA), X-ray diffractometry (XRD), scanning electron microscopy (SEM), mechanical and chemical resistance measurements. It was found that in CaF_2 containing samples, the sinterability, crystallization and mechanical properties were improved by increasing of CaF_2 amount. However, addition of ZrO_2 and TiO_2 increases the firing temperature required for complete densification of specimens. Our experiments showed that fluctuations of chemical composition of the residual glass phases during sintering were responsible for these dissimilar trends and greatly influenced mechanical and chemical properties. According to the obtained results, appropriate sinterability, acceptable mechanical and chemical properties, as well as desirable whiteness of the most promising specimens make them suitable choices for floor tile applications. The main crystallization phases in all fully sintered glass–ceramics were wollastonite, anorthite and calcium aluminum silicate.

1. Introduction

Glass–ceramics can be obtained either by heat treatment of a preformed glass article or by sintering route [1–3]. In the case of sintered glass–ceramics, if crystallization occurs before densification, the viscosity of samples will be increased. It is due to the contribution of glass composition into a crystalline phase structure, resulting in reduction of viscous flowing of system. As a result, densification through viscous flow sintering will not occur properly and a porous body will be formed [4–9].

According to previous experiments, glass powders with surface crystallization tendency are more suitable for sintering rather than those which are crystallized through bulk mechanism [10–12]. In the former case, viscous flow occurs more effectively rather than crystallization, which makes the compacted glassy powders more susceptible for sintering. Since surface crystallization is predominant in the $CaO–Al_2O_3–SiO_2$ glasses, sintering seems to be a suitable method for preparation of related glass–ceramics. On the other hand, the ability to precipitation of hard crystalline phases, e.g. wollastonite ($CaO{\cdot}SiO_2$) with hardness of 4.5–5 Mohs and anorthite ($CaO{\cdot}Al_2O_3{\cdot}2SiO_2$) with hardness of 6 Mohs in this ternary system, as well as abundant and economical raw materials (i.e. calcium carbonate, kaolin, etc.) make it favorable for different applications such as building glass–ceramics, floor tiles, claddings, etc. [2].

To facilitate crystallization in this ternary system, different nucleating agents have been employed. Titanium oxide (TiO_2) is an effective nucleating agent which is widely used in this system [2,3,12]. It is believed that this oxide is greatly dissolved in glass melts; however, due to its high ionic field strength encourages the liquid–liquid phase separation phenomenon during subsequent heat treatment of solid glass [2,3]. During cooling it can precipitate in the forms of titanium oxide or titanium compounds and facilitate development of main crystalline phases by acting as a nucleant [2,3]. Zirconium oxide (ZrO_2) and fluoride compounds are also used as nucleating agents. Fluorides improve crystallization through reduction of viscosity of glass phase [11–15]. However, sometimes precipitation of fine compounds of these materials in the form of ZrO_2 or CaF_2 nuclei renders heterogeneous nucleation sites and improves crystallization [3,12–15]. The role of precipitated tetragonal zirconium oxide in development of crystallization has also been reported [3,16].

Other nucleating agents such as Cr_2O_3 and Fe_2O_3 have been used in this ternary system [1]. But unlike Cr_2O_3 and Fe_2O_3, which have been greatly used as nucleating agents in this system, the above-mentioned nucleants (TiO_2, ZrO_2 and fluorides) do not decline the whiteness of final products and provide extensive possibility to decorate final products. Furthermore, the effects of as-mentioned materials on crystallization, sinterability, mechanical and chemi-

* Corresponding author. Tel.: +98 21 73912873; fax: +98 21 77240480.
E-mail addresses: banijamalis@metaleng.iust.ac.ir (S. Banijamali), beftekhari@iust.ac.ir (B. Eftekhari Yekta), hrezaie@iust.ac.ir (H.R. Rezaie), vmarghus@iust.ac.ir (V.K. Marghussian).

0040-6031/$ – see front matter © 2009 Elsevier B.V. All rights reserved.
doi:10.1016/j.tca.2008.12.031

cal properties of sintered $CaO–Al_2O_3–SiO_2$ glass–ceramics have not been well documented.

Hence, the nucleating ability and the effects of various amounts of titanium oxide, zirconium oxide and calcium fluoride on crystallization and sintering behavior of this system glasses were considered in this work. Furthermore, mechanical and chemical resistance measurements were performed to evaluate the possibility of using optimized samples as building glass–ceramics.

2. Experimental procedure

Raw materials were chosen from commercial grade calcium carbonate, corundum, silicon oxide, titanium oxide, zirconium oxide and calcium fluoride. The homogenized mixture of raw materials was transferred to a zircon crucible and melted at 1450 °C for 1 h in an electric furnace. The melts were water quenched and the obtained frits were dried and milled to the required particle sizes (<75 μm). Particle size distributions of glass powders were characterized by a laser particle size analyzer (Fritsch analysette 22).

Table 1 shows the chemical composition of glasses. It should be noted that the glass ST22 was considered as the start up composition [2]. The amount of TiO_2 in this composition was considerably more than what is commonly used in glass–ceramic technology as a nucleating agent. Hence its gradual reduction in glass composition and using other nucleating agents were considered in this work. During melting, only molten glasses SF6, SF9, SF12, SZ6, ST6, ST9 and ST22 were flow-able under the selected condition. Therefore, just the mentioned compositions were selected for the subsequent steps.

0.2 wt.% CMC (carboxy methyl cellulose), based on glass powder weight, was added to the obtained powders as a binder. Compacted powders were obtained by uniaxially pressing at 30 MPa in 20 mm cylindrical die. These compacts were then sintered systematically in an electric furnace at 850 up to 1200 °C. Firing were carried out at a heating rate of 7 °C min^{-1} for 1 h at maximum temperature. Then the furnace was allowed to cool down to room temperature. Linear shrinkage and water absorption [17] were measured to evaluate sintering behavior. The thermal behavior of the glasses was monitored by differential thermal analyzer (Netzsch 404) at a heating rate of 10 °C min^{-1} in air. Alumina was used as the reference material and the condition of atmosphere control was static. Precipitated crystalline phases in the sintered samples were identified by using X-ray diffractometers (Siemens-D500 and JEOL JDX-8030). The chemical resistance of the glass–ceramics was examined according to the modified [18] standard. To measure chemical resistance of sintered specimens, they were put in an acidic solution of H_2SO_4 and boiled for 1 h. The weight difference before and after this chemical leaching was considered as an evidence for chemical resistance measurement. The microhardness of each glass–ceramic was measured by a Vickers tester (Buehler, Micromete 1) with an indentation load of 100 gf (gram-force) for 30 s. The average value was obtained from 10 indentations. Bending strength was measured according to the three point bending test [19] using MTS machine (10/M) at a cross-head speed of 0.6 mm min^{-1}. The average value was obtained from measurement of five samples.

The microstructures of the sintered samples were evaluated by scanning electron microscope (Cambridge-S360) after polishing and etching in 5% HF solution for 15 s.

Table 1
Chemical composition of glasses (weight part).

Glass composition	CaO	Al_2O_3	SiO_2	TiO_2	ZrO_2	CaF_2
S	23.53	42.84	33.63	–	–	–
ST3	23.53	42.84	33.63	3	–	–
ST6	23.53	42.84	33.63	6	–	–
ST9	23.53	42.84	33.63	9	–	–
ST22[a]	23.53	42.84	33.63	22	–	–
SZ3	23.53	42.84	33.63	–	3	–
SZ6	23.53	42.84	33.63	–	6	–
SZ9	23.53	42.84	33.63	–	9	–
SZ12	23.53	42.84	33.63	–	12	–
SF3	23.53	42.84	33.63	–	–	3
SF6	23.53	42.84	33.63	–	–	6
SF9	23.53	42.84	33.63	–	–	9
SF12	23.53	42.84	33.63	–	–	12

[a] Chosen from reference.

3. Results and discussion

3.1. DTA analysis

Fig. 1 shows the results of DTA analysis of the glasses. It can be realized that in TiO_2 bearing specimens, crystallization peak temperature increases with increasing TiO_2 amount. However, increasing of TiO_2 amount decreased glass viscosity of specimens during melting. It seems that incomplete melted compounds in ST6 and ST9 act as seeds and reduce the crystallization peak temperature of these glasses rather than completely melted ST22.

On the other hand, in fluorine containing specimens, increasing of fluorine content led to reduction of the first crystallization peak temperature which is due to the formation of wollastonite,

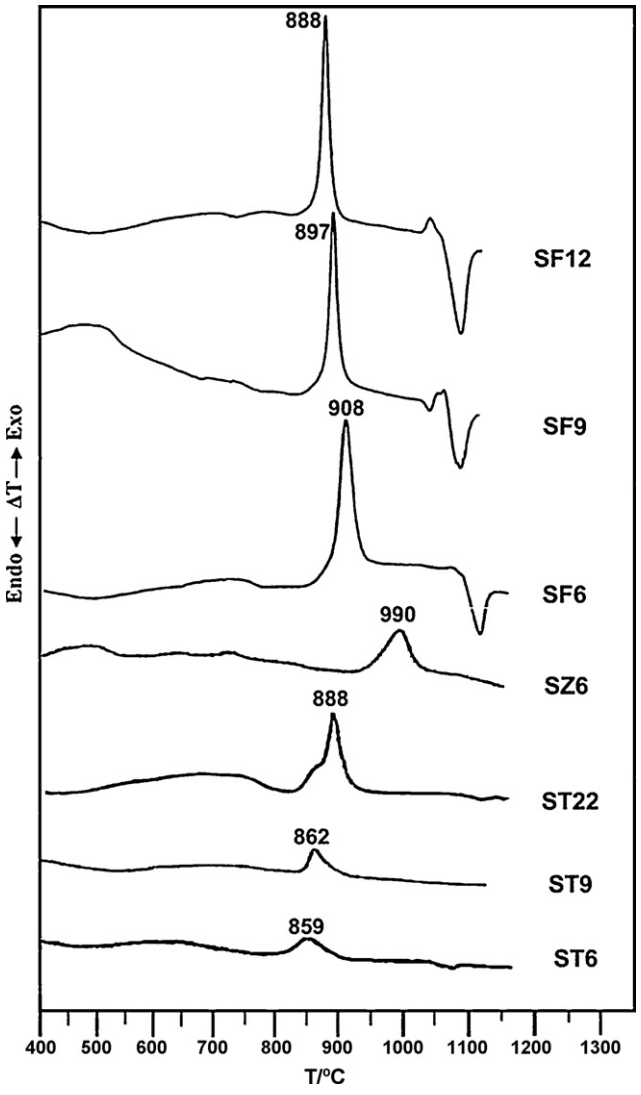

Fig. 1. DTA profiles of glass samples (<75 μm) at a heating rate of 10 °C min^{-1}.

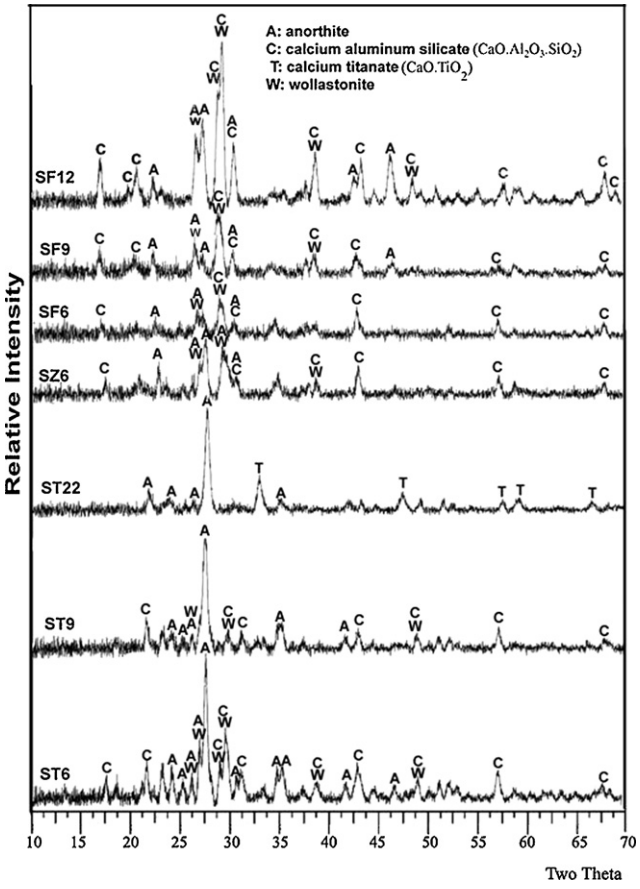

Fig. 2. XRD patterns of glass samples heat treated at their main crystallization peak temperature for 1 h.

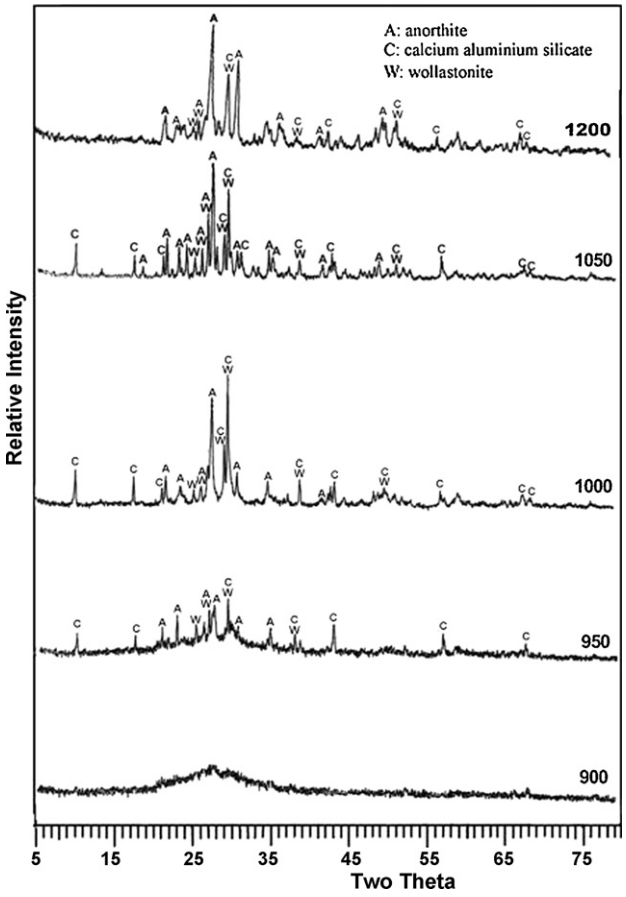

Fig. 3. XRD patterns of sample SZ6 after sintering at various temperatures.

anorthite and calcium aluminum silicate phases. Fluorine facilitates crystallization through weakening structural glass bonds, so decreases viscosity [12–14]. Furthermore, in SF9 and SF12 samples a small second exothermic peak can be observed at about 1050 °C which was attributed to the formation of gehlenite ($2CaO{\cdot}Al_2O_3{\cdot}SiO_2$) according to the XRD results. There is also a sharp endothermic peak at about 1150 °C in each CaF_2 bearing sample which is absent in the other DTA profiles. This peak was attributed to the liquidus temperature or melting temperature of crystalline phases. If the specimens were heated at this temperature, a considerable volume of glass melt will be formed in them.

It is obvious that glass SZ6 is crystallized at the highest temperature. Since no form of zirconium compounds was observed in the XRD patterns (Figs. 2 and 3), Zr^{4+} ions should be remained dissolved in the glassy phase. Since zirconium ion enhances the viscosity of glass [1–3], it can be responsible for the shifting of the crystallization peak temperature to the higher temperature.

3.2. XRD analysis

Fig. 2 shows the XRD patterns of specimens after heat treatment at their main crystallization peak temperature. According to these results, calcium titanate ($CaO{\cdot}TiO_2$) and anorthite in ST22; and wollastonite, calcium aluminum silicate ($CaO{\cdot}Al_2O_3{\cdot}SiO_2$) and anorthite in the other samples are the main crystalline phases which precipitate at the crystallization temperature. It should also be mentioned that XRD analysis of as-quenched ST6 and ST9 frits showed the presence of un-melted particles of wollastonite, anorthite and calcium aluminum silicate ($CaO{\cdot}Al_2O_3{\cdot}SiO_2$) (Fig. 4). These particles had been formed apparently through solid-state reactions of raw materials during melting procedure. Accordingly, F^- and Zr^{4+} ions have been remained dissolved in the residual glass phase of the fluoride and zirconium oxide containing glasses and do not contribute in the formation of any crystalline phases. Similar to the DTA thermographs, the intensity of crystalline phases in fluorine containing samples increases by increasing of CaF_2 amount.

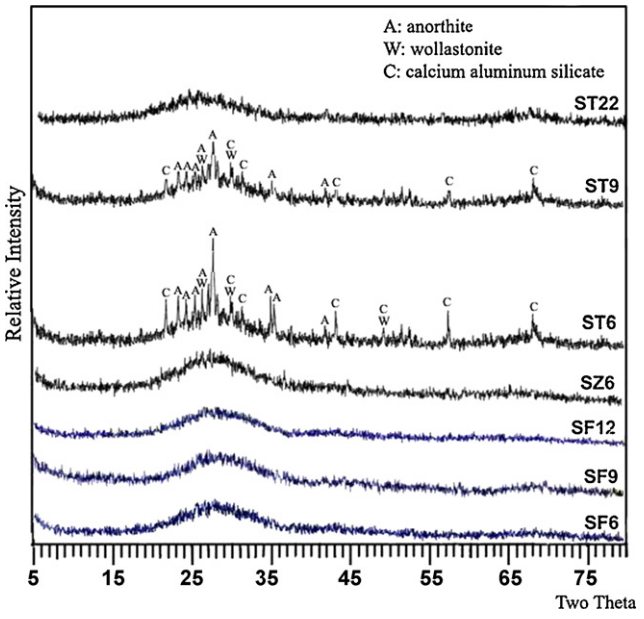

Fig. 4. XRD patterns of as-quenched frits.

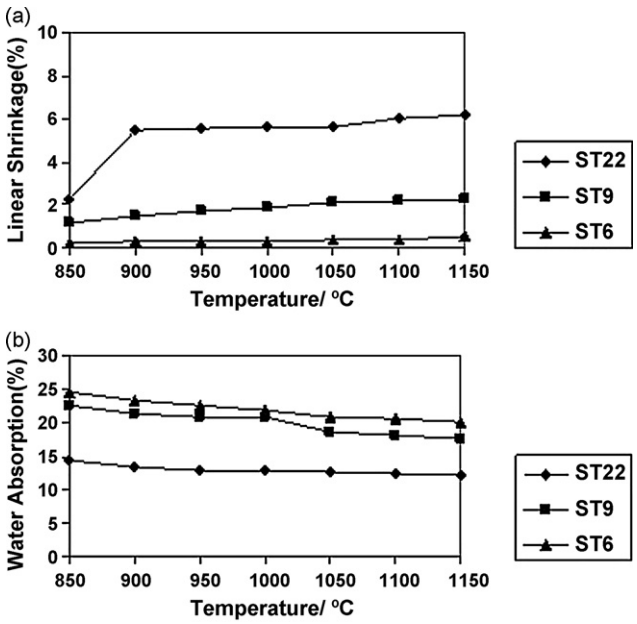

Fig. 5. Sintering behavior of TiO_2 containing specimens versus temperature as (a) linear shrinkage and (b) water absorption.

Fig. 3 shows phase evolution of zirconium oxide containing specimen during sintering. It can be seen that wollastonite and calcium aluminum silicate start to dissolve into the glass matrix around 1050 °C. It is obvious that calcium aluminum silicate has completely dissolved in the matrix at about 1200 °C. (Phase evolution of fluorine containing specimens during sintering had been investigated in previous work in details [20].)

3.3. Sintering behavior

Figs. 5–7 depict the linear shrinkage (%) and water absorption (%) of glasses during sintering. As it was expected, the sinterability of

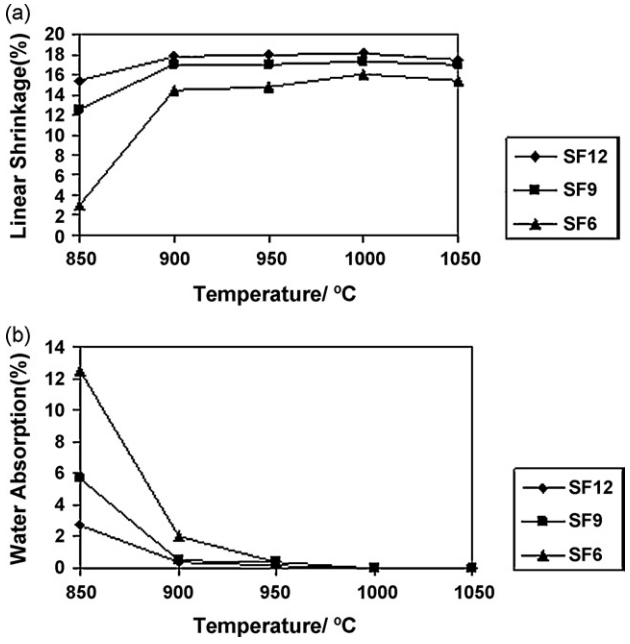

Fig. 6. Sintering behavior of CaF_2 containing specimens versus temperature as (a) linear shrinkage and (b) water absorption.

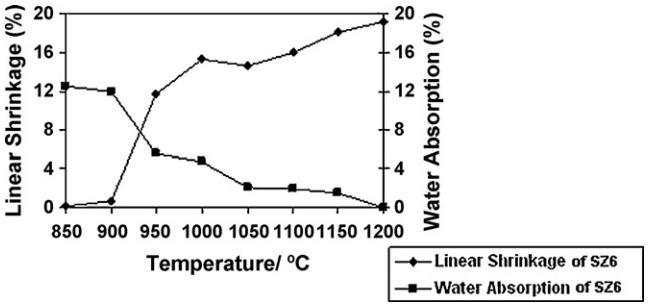

Fig. 7. Sintering behavior of ZrO_2 containing specimen versus temperature.

TiO_2 bearing glasses was destroyed by decreasing of TiO_2 amounts. As mentioned earlier, TiO_2 acts as a flux in this system and improves the densification of glasses. However, even in the best condition, i.e. ST22, the sinterability of these glasses was weaker than the ZrO_2 and CaF_2 containing specimens. It can be observed that the water absorption of ST22 is as high as 15 wt.% after firing at 1150 °C. By considering the XRD patterns (Fig. 2) and sintering behavior of ST22 (Fig. 5), it seems that the formation of calcium titanate leads to depletion of the residual glass phase from strong fluxes such as CaO and TiO_2. As a result, the viscosity of the residual glass phase increases gradually during crystallization and causes unfavorable sinterability.

The viscosity of the residual glass phase of sample SZ6 also increases during crystallization, but via an opposite procedure, in which promotion of crystallization leads to gradual enrichment of glassy phase with the refractory Zr element. This condition rises the firing temperature, required for obtaining a fully dense specimen, up to 1200 °C (Fig. 7).

In our previous work [20], it was found that in fluorine bearing samples, fluorine remains in the residual glass after crystallization. Gradually enrichment of the residual glass phase with a powerful flux like fluorine compensates extensive crystallization in these samples and insures their complete densification at temperatures as low as 1000 °C (Fig. 6).

3.4. Microstructural evaluation

Figs. 8 and 9 show the SEM micrographs of sintered glass–ceramics (micrographs obtained by secondary and back-scattered electrons have been labeled by SE and BS, respectively).

In the CaF_2 bearing glasses, the chain-like lines which are consisted of small white spheres, distributed around the glass particles, confirm initiation of crystallization from the surface of each glass particle. (Surface crystallization areas have been shown by dash lines in Fig. 8.)

Furthermore, by increasing fluorine content, microstructure of specimens becomes finer. This phenomenon is well matched by related DTA thermographs. According to the DTA results, by increasing fluorine content, the crystallization peak temperature decreases which is responsible for more effective nucleation, probably via acceleration of diffusion rate of crystalline phase constituents. On the other hand, sintered SZ6 glass–ceramic reveals a coarser microstructure in which the needle-like crystals have been extended from the surface toward the center of glass particles. This behavior has led to the crack-like defects in the middle of particles, which have been marked by black arrows in Fig. 9b. According to the authors' opinion, a considerable lower density of initial glass phase (compared to the density of precipitated crystalline phases) creates noticeable voids at the center of the glass particles, where the crystallite-ends reach together. Due to the fact that the viscosity of the residual glass phase is not low enough to fill interconnected voids, these voids will be remained and form crack-like defects in

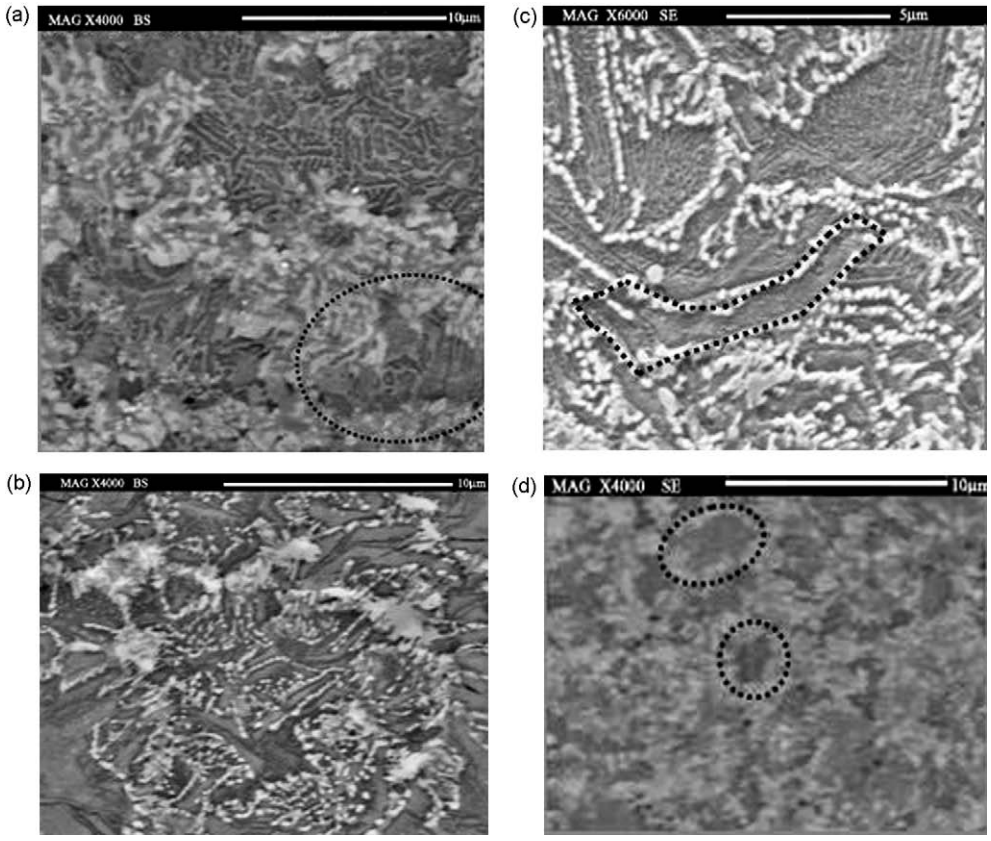

Fig. 8. SEM micrographs of fluorine containing specimens sintered at 1000 °C for 1 h (surface crystallization has been shown by dash lines): (a) SF6, (b) SF9 (4000×), (c) SF9 (6000×), and (d) SF12.

the middle of the glass particles. The coarsening of microstructure is also attributed to the higher crystallization temperature and postponed densification of sample SZ6.

3.5. Mechanical and chemical properties

Table 2 shows the mechanical properties and chemical resistance of fully dense sintered glass–ceramics. As it was discussed previously [20], increasing of fluorine amounts promotes mechanical properties and degrades chemical resistance in fluorine containing samples.

According to the obtained results, in spite of less crystallization in SZ6 (Figs. 1 and 2), this sample shows the highest Vickers hardness and improved chemical resistance rather than fluorine containing specimens. Since the crystalline phases in these two different glass–ceramics are the same, these observations confirm

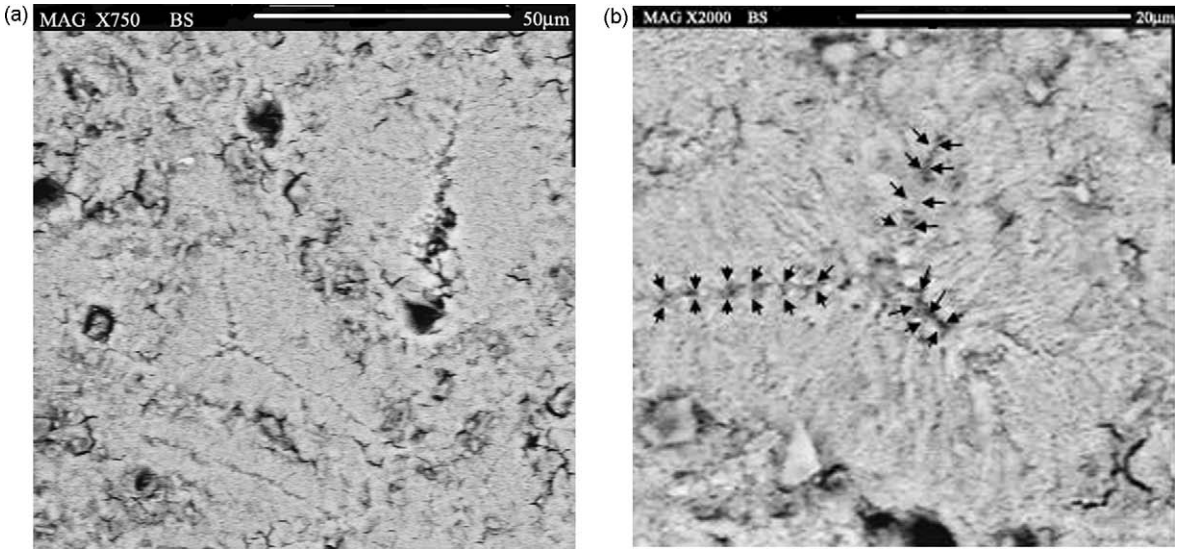

Fig. 9. SEM micrographs of SZ6 sample sintered at 1000 °C for 1 h (crack-like defects have been shown by black arrows in the middle of a grain): (a) 750 magnification and (b) 2000 magnification.

Table 2
Mechanical and chemical properties of sintered glass–ceramics.

Properties	SZ6	SF6	SF9	SF12
Vickers hardness (VHN)	613	540	564	595
Bending strength (MPa)	74	107	123	128
Weight loss (%)	1.8	2.07	2.20	2.28

again the effective role of the residual glass composition on the above-mentioned properties. Apparently, the presence of Zr^{4+} ions in the residual glass network makes it strong enough that compensates poor crystallization in point of hardness view. However, bending strength of SZ6 is considerably lower than the other sintered specimens which is probably related to the less crystallization and lack of various strengthening mechanisms (like crack pinning, crack deflection, etc.), consequently. Furthermore, coarser structure and existence of crack-like defects (Fig. 9) are responsible for this matter.

4. Conclusions

Applying TiO_2, CaF_2 and ZrO_2 in the investigated glasses led to different results in points of crystallization, sintering, mechanical and chemical properties views. While gradually addition of CaF_2 into the base glass improved the sinterability, crystallization, and mechanical properties of the specimens, the two other nucleants did not show the as-mentioned trend.

It was found that mechanical and chemical properties are mostly affected by the composition of the residual glass as well as crystallinity and inherence of crystalline phases. In titanium oxide bearing glasses, depletion of residual glass phase from calcium and titanium ions and in the zirconium one enrichment of glassy phase by zirconium ion make them viscous enough to prevent their complete densification. The residual glass phase in the CaF_2 containing glasses became more flow-able by increasing dissolved F^- ions, which caused the samples to be more sinterable and crystallized.

Microstructural analysis showed that surface crystallization was the dominant mechanism of crystallization of sintered glass–ceramics. In zirconium bearing glass, surface crystallization in cooperation with a low density (compared to crystalline phases) and viscous glassy phase caused crack-like defects in this specimen which led to its lower bending strength.

With respect to mechanical properties and chemical resistance measurements, fully sintered glass–ceramics (SF6, SF9, SF12 and SZ6) seem to be suitable choices for application as floor tiles. Although densification of SZ6 sample occurs at higher temperature (near 1200 °C), it is still compatible with firing schedule of porcelain tiles.

References

[1] W. Holland, G. Beall, Glass–Ceramic Technology, American Ceramic Society, OH, 2002.
[2] Z. Strnad, Glass–Ceramic Materials, Elsevier, New York, 1986.
[3] P.W. MacMillan, Glass–Ceramics, Academic Press, New York, 1979.
[4] C. Siligardi, M.C. D'Arrigo, C. Leonelli, Am. Ceram. Soc. Bull. 79 (2000) 88–92.
[5] M. Aloisi, A. Karamanov, M. Pelino, J. Non-Cryst. Solids 345 (2004) 192–196.
[6] A. Karamanov, M. Aloisi, M. Pelino, J. Eur. Ceram. Soc. 25 (2005) 1531–1540.
[7] M. Karamanov, M. Salvo, I. Metecovits, J. Eur. Ceram. Soc. 23 (2003) 1609–1615.
[8] D.U. Tulyaganov, M.J. Ribeiro, J.A. Labrinch, Ceram. Int. 28 (2002) 515–520.
[9] C. Lira, A.P. Oliveira, O.E. Alarcon, Glass Technol. 42 (2001) 91–96.
[10] M.E. Rabinovich, J. Mater. Sci. 20 (1985) 4259–4297.
[11] K. Sujirote, R.D. Rawlings, P.S. Rogers, J. Eur. Ceram. Soc. 18 (1998) 1325–1330.
[12] S.N. Salama, S.M. Salman, H. Darwish, Ceram-Silicaty 46 (2002) 15–23.
[13] H. An-Min, L. Kai-Ming, P. Fei, W. Guo-Liang, S. Hua, Thermochim. Acta 413 (2004) 53–55.
[14] J.A. Griggs, K.J. Anusavice, J.J. Mecholsky, J. Mater. Sci. 37 (2002) 2017–2022.
[15] E.Y. Guseva, M.N. Gulyukin, Inorg. Mater. 38 (2002) 962–965.
[16] P. Loiseau, D. Caurant, O. Majerus, N. Baffier, J. Mater. Sci. 38 (2003) 853–864.
[17] EN ISO 10545-3 1997, Ceramic tiles—Part 3. Determination of water absorption, apparent porosity, apparent relative density and bulk density (ISO 10545-3:1995, including Technical Corrigendum 1:1997).
[18] EN ISO 10545-13 1997, Ceramic tiles —Part 13. Determination of chemical resistance (ISO 30545-13:1995).
[19] ASTM C 158-95 2000, Standards test methods for strength of glass by flexure (determination of modulus of rupture).
[20] S. Banijamali, B. Eftekhari Yekta, H.R. Rezaie, V.K. Marghussian, Adv. Appl. Ceram. 107 (2008) 101–105.